

Forum "Redox Translational Medicine"

Forum Article

Title: Glucose acutely reduces cytosolic and mitochondrial H₂O₂ in rat pancreatic beta-cells.

Authors: Jean-Philippe Deglasse¹, Leticia Prates Roma^{2,3}, Daniel Pastor-Flores², Patrick Gilon¹, Tobias P. Dick², Jean-Christophe Jonas¹

Affiliations:

¹ Université catholique de Louvain, Institute of experimental and clinical research, Pole of endocrinology, diabetes and nutrition, Brussels, Belgium, B-1200

² Division of Redox Regulation, DKFZ-ZMBH Alliance, German Cancer Research Center (DKFZ), 69120 Heidelberg, Germany

³Department of Biophysics, Center for Human and Molecular Biology, Saarland University, 66421 Homburg, Germany

Abbreviated title: Glucose decreases pancreatic beta-cell H₂O₂

Address correspondence to:

Jean-Christophe Jonas

UCL/SSS/IREC/EDIN

Avenue Hippocrate 55, B1.55.06

B-1200 Brussels

Telephone: +32 2 764 95 75

E-mail: jean-christophe.jonas@uclouvain.be

Manuscript keywords (3-6 search terms): hydrogen peroxide; HyPer probe, insulin secretion; menadione; roGFP probe; pancreatic islet

Abstract

Aims: Whether H₂O₂ contributes to the glucose-dependent stimulation of insulin secretion by pancreatic β -cells is highly controversial. We used two H₂O₂-sensitive probes, roGFP2-Orp1 and HyPer with its pH-control SypHer, to test the acute effects of glucose, monomethylsuccinate, leucine with glutamine, and α -ketoisocaproate, on β -cell cytosolic and mitochondrial H₂O₂ concentrations. We then tested the effects of low H₂O₂ and menadione concentrations on insulin secretion.

Results: RoGFP2-Orp1 was more sensitive than HyPer to H₂O₂ (response at 2-5 vs. 10 μ M) and less pH-sensitive. Under control conditions, stimulation with glucose reduced mitochondrial roGFP2-Orp1 oxidation without affecting cytosolic roGFP2-Orp1 and HyPer fluorescence ratios, except for the pH-dependent effects on HyPer. However, stimulation with glucose decreased the oxidation of both cytosolic probes by 15 μ M exogenous H₂O₂. The glucose effects were not affected by overexpression of catalase, mitochondrial catalase or superoxide dismutase 1 and 2. They followed the increase in NAD(P)H autofluorescence, were maximal at 5mM glucose in the cytosol and 10mM glucose in the mitochondria, and were partly mimicked by the other nutrients. Exogenous H₂O₂ (1-15 μ M) did not affect insulin secretion. By contrast, menadione (1-5 μ M) did not increase basal insulin secretion but reduced the stimulation of insulin secretion by 20mM glucose.

Innovation: Subcellular changes in β -cell H₂O₂ levels are better monitored with roGFP2-Orp1 than HyPer/SypHer. Nutrients acutely lower mitochondrial H₂O₂ levels in β -cells and promote degradation of exogenously supplied H₂O₂ in both cytosolic and mitochondrial compartments.

Conclusion: The glucose-dependent stimulation of insulin secretion occurs independently of a detectable increase in β -cell cytosolic or mitochondrial H₂O₂ levels.

List of abbreviations

Ad-“gene”: adenovirus coding a specific gene under the control of the CMV promoter

Ad-Null, empty vector adenovirus

AT2, aldrithiol

[Ca²⁺]_c, free cytosolic Ca²⁺ concentration

Cat, catalase

CMV, cytomegalovirus

DTT, dithiothreitol

GFP, green fluorescent protein

Gn, n mM glucose

GSIS, glucose-dependent stimulation of insulin secretion

HyPer, Hydrogen Peroxide sensor

KIC, α-ketoisocaproate

KRB, bicarbonate-buffered Krebs solution

MMS, monomethyl succinate

mt-, mitochondria-targeted

(mt-)roGFP2-Orp1, untargeted or mitochondria-targeted roGFP2-Orp1

Orp1, Oxidant receptor peroxidase 1

OxD, oxidation ratio

RIP, rat insulin promoter

roGFP2, reduction-oxidation sensitive enhanced GFP

roGFP2-Orp1, roGFP2 fused to Orp1

SOD, superoxide dismutase

SypHer, HyPer-derived pH probe

Introduction

The glucose-dependent stimulation of insulin secretion (GSIS) by pancreatic β -cells, which plays a central role in blood glucose homeostasis, results from an acceleration of glycolysis and the mitochondrial Krebs cycle, with an increased production of several metabolic coupling factors (36,50). Among these, the rise in cytosolic ATP to ADP ratio closes K_{ATP} channels, leading to plasma membrane depolarization, an influx of Ca²⁺ and insulin granule exocytosis. Other metabolic coupling factors enhance the Ca²⁺ influx, amplify its efficacy on exocytosis or directly increase exocytosis, thereby contributing to the triggering and metabolic amplification of insulin secretion.

Both NADPH and H₂O₂ are putative metabolic coupling factors involved in GSIS. However, the evidence is stronger for a role of NADPH than H₂O₂. There is no doubt that glucose increases the NADPH/NADP⁺ ratio in β -cells (5,13), and there is good evidence that NADPH plays a permissive role in Ca²⁺-induced exocytosis by a mechanism requiring glutaredoxin 1 and possibly involving sentrin/small ubiquitin-like modifier-specific protease 1 (10,15,39). Regarding H₂O₂, the rationale for its role in GSIS stems from the low expression of classical antioxidant enzymes in β -cells (19) and from the observation that low concentrations of H₂O₂ stimulate the influx of Ca²⁺ and insulin secretion at non-stimulating glucose concentrations, while antioxidant drugs inhibit GSIS (18,33). Consequently, it was postulated that an increase in β -cell antioxidant defenses would not only reduce β -cell oxidative stress but also be detrimental to GSIS (34). However, the role of H₂O₂ in GSIS remains controversial for several reasons. First, the concentration of H₂O₂ and other reactive oxygen species in β -cells stimulated with glucose was shown to either increase (4,18,30) or decrease (24,43) depending on the experimental system or measurement technique. Second, increasing the expression of H₂O₂-degrading enzymes did not negatively affect GSIS while affording protection against H₂O₂ toxicity (21,25), and inactivating NADPH oxidase 2 increased acute GSIS by isolated mouse islets (8,20). Finally, the concept that β -cells have low antioxidant defenses was recently challenged by the observation that, upon exposure to exogenous H₂O₂, β -cell cytosolic H₂O₂ increased only after cytosolic NADPH had markedly decreased, suggesting that provision of NADPH to the antioxidant system is a critical determinant of β -cell antioxidant defenses (5). In favor of the latter hypothesis, we previously showed that glucose acutely decreases mitochondrial glutathione oxidation in rodent and human β -cells, and that this effect is correlated with the rise in mitochondrial NADPH (42,48).

As NADPH drives the enzymatic degradation of H₂O₂, it seems unlikely that NADPH and H₂O₂ could both stimulate insulin secretion unless their increases are spatially or temporally disconnected. Therefore, to test whether H₂O₂ can act as a metabolic coupling factor in GSIS, we used two genetically-encoded H₂O₂-sensitive fluorescent probes, roGFP2-Orp1 and HyPer with its pH-control

probe SypHer (1,12,26,29,35), and monitored changes in cytosolic and mitochondrial H₂O₂ concentrations in rat islet β -cells acutely stimulated with glucose and monomethylsuccinate (MMS), a combination of leucine and glutamine (Leu/Gln) or α -ketoisocaproate (KIC). To sensitize our experimental system to small effects of these nutrients on cytosolic H₂O₂ concentrations, we also tested their effects on the oxidation of the probes by low concentrations of exogenous H₂O₂. Finally, we also tested the effect of low concentrations of H₂O₂ and of menadione, a quinone that produces superoxide mainly in the mitochondria through futile redox cycling by oxidoreductases (7), on insulin secretion at non-stimulating and stimulating glucose concentrations. Our results do not support the hypothesis that a rise in H₂O₂ is involved in GSIS. Instead, they show that, despite the low expression of classical antioxidant enzymes in β -cells, glucose, MMS, Leu/Gln and KIC acutely reduce endogenous and exogenous H₂O₂ in their mitochondrial matrix and cytosol.

Results

Expression of (mt-)roGFP2-Orp1 and HyPer/SypHer in rat islet cells - Rat islet cell clusters were co-infected with an adenovirus coding roGFP2-Orp1 or mt-roGFP2-Orp1 under the control of the cytomegalovirus (CMV) promoter (Ad-(mt-)roGFP2-Orp1) and an adenovirus coding the red fluorescent protein DsRed under the control of the rat insulin promoter (Ad-RIP-DsRed) to identify β -cells. Two days later, about 75% of the cells expressed DsRed, more than 81-88% expressed the H₂O₂-sensing probe, and 72% expressed both fluorescent proteins (Fig. 1A-B and Table 1). In whole rat islets infected for two days with Ad-RIP-DsRed and either Ad-HyPer or Ad-SypHer, confocal microscopy revealed that the probes were only expressed at the islet periphery where the proportion of β -cells is lower (Fig. 1C-D). Nevertheless, more than two thirds of cells expressing the probes were also DsRed-positive (Table 1). These results confirm that, despite the use of the CMV promoter, adenovirus-mediated gene expression preferentially targeted β -cells over other islet cell types (41,48). The changes in probe fluorescence ratio reported hereafter should therefore mainly reflect what happens in β -cells. We also checked the subcellular localization of the probes by confocal microscopy. Figure 1C-F shows that HyPer, SypHer and roGFP2-Orp1 were expressed in the cytosol and nucleus of islet cells, whereas mt-roGFP2-Orp1 was expressed in mitochondria.

Effects of H₂O₂, menadione, glucose and pH on (mt-)roGFP2-Orp1 fluorescence ratio in rat islet cells - In the presence of 5 or 10mM glucose (G5 or G10), the initial normalized fluorescence ratio of roGFP2-Orp1 was lower in the cytosol than in the mitochondrial matrix (Fig. 2B-C and K-L), in agreement with our previous observations using roGFP1 and GRX1-roGFP2 (roGFP2 fused to glutaredoxin 1) (41,48). As expected, exogenous H₂O₂ dose-dependently and reversibly increased the normalized fluorescence ratio of roGFP2-Orp1 in both compartments (Fig. 2A-D and K-M). These

effects were observed within minutes of exposure to H₂O₂ at concentrations that were lower than the concentration (50μM) required to alter islet-cell survival and secretory function during 24h of culture (16). In the presence of G10, this effect was significant at 5μM H₂O₂ in the cytosol and at 10μM H₂O₂ in the mitochondrial matrix. In the presence of G5, it was significant at 2μM H₂O₂ in the cytosol and at 5μM H₂O₂ in mitochondria. In both compartments, the amplitude of probe oxidation by 10μM H₂O₂ was larger in G5 than G10. At the periphery of whole islets, roGFP2-Orp1 was also more sensitive to exogenous H₂O₂ in the cytosol than in the mitochondrial matrix (Fig. 2E and N). By contrast, it was less oxidized in the cytosol than in the mitochondria in response to menadione (Fig. 2J and R).

We next tested the acute effects of glucose on mitochondrial and cytosolic roGFP2-Orp1. In comparison with clusters perfused in KRB containing G10 throughout the experiment, the mt-roGFP2-Orp1 fluorescence ratio increased when glucose was lowered from G10 to G2, and decreased upon subsequent stimulation with G30 (Fig. 2O), indicating that glucose acutely reduced mitochondrial H₂O₂ concentration in islet cells. These effects of glucose were similar in clusters in which the expression of catalase targeted to mitochondria protected mt-roGFP2-Orp1 from its oxidation by 15μM H₂O₂ (Fig. 3C-D, F, K-L). Interestingly, changes of similar direction but lower amplitude were observed between G10, G4 and G7 (Fig. 2P), indicating the physiological relevance of this glucose effect.

In contrast to the mitochondrial probe, the normalized fluorescence ratio of cytosolic roGFP2-Orp1 was affected by less than 1% between G2 and G30 (Fig. 2F), and this lack of glucose effect was confirmed in clusters infected with both Ad-SOD1 and Ad-SOD2 (Fig. 3A, G, H, M-P). However, in the presence of 15μM exogenous H₂O₂, the oxidation of roGFP2-Orp1 increased when glucose was lowered from G10 to G0.5, then decreased upon stimulation with G30 (Fig. 2G). In clusters overexpressing catalase (Fig. 3E and I-J), the increase in roGFP2-Orp1 fluorescence ratio elicited by 15 μM H₂O₂ was reduced by 60% but the glucose effect was proportionally preserved (Fig. 3B). Also in the presence of 5μM H₂O₂, roGFP2-Orp1 oxidation progressively increased upon stepwise reduction in glucose from G10 to G5, G2 and G0.5 (Fig. 2H). These results show that glucose does not increase cytosolic H₂O₂ under control conditions, even in the presence of SOD1 and 2 that should favor H₂O₂ production from superoxide. In contrast, they suggest that glucose improves the β-cell ability to degrade H₂O₂.

Like enhanced-GFP, roGFP2-derived probes are slightly pH-sensitive (26). As the stimulation of β-cells with glucose acutely alkalinizes the mitochondrial matrix and, to a lesser extent, the cytosol (44,49), we checked the sensitivity of (mt-)roGFP2-Orp1 to changes in pH. As shown in Figure 2 I and Q, the fluorescence ratio of each probe was almost unaffected by 30mM Na-acetate and was slightly

increased upon addition of 30mM NH₄Cl. The decrease of the (mt-)roGFP2-Orp1 fluorescence ratio by glucose was therefore unrelated to its alkalizing action in β -cells.

Effects of H₂O₂ and glucose on HyPer/SypHer fluorescence ratios in rat islet cells – Besides roGFP2-Orp1, HyPer can also be used to measure changes in β -cell H₂O₂ concentration (1,9). However, the high pH sensitivity of HyPer imposes the use of a pH control probe like SypHer, a HyPer-derived probe that is identically affected by pH but insensitive to H₂O₂ (35). We have previously shown that, in the mitochondrial matrix of rat β -cells, the glucose-induced changes in the HyPer fluorescence ratio resemble those of SypHer and result from the strong alkalizing action of glucose in that compartment (41). In whole rat islets perfused at G10, the fluorescence ratio of cytosolic HyPer significantly increased upon addition of 20 μ M H₂O₂ or 30mM NH₄Cl, while that of SypHer only increased in response to NH₄Cl (Fig. 4A). The fluorescence ratios of both probes were therefore compared after normalization of the traces to the initial fluorescence ratio measured in G10 set to 0%, and to the peak ratio in the presence of NH₄Cl set to 100%. Figure 4B shows that, except for the lack of response of SypHer to H₂O₂, the glucose-induced changes in HyPer fluorescence ratio were almost identical to those of SypHer, indicating that they were due to changes in intracellular pH. Similar results were observed in the presence of 20mM HEPES (Fig. 4D-E), except for the lower amplitude of glucose-induced changes in cytosolic pH. However, in the presence of 15 μ M H₂O₂, which increased the HyPer (but not the SypHer) normalized fluorescence ratio by about 20% in G10, the HyPer fluorescence ratio increased when glucose was lowered from G10 to G0.5, and decreased upon subsequent stimulation with G5 and G30, while the SypHer fluorescence ratio was only slightly affected (Fig. 4C). These results confirm that glucose does not detectably increase cytosolic H₂O₂ in β -cells but rather promotes the β -cell ability to degrade H₂O₂.

Effects of H₂O₂ and glucose on NADPH and (mt-)roGFP2-Orp1 fluorescence ratio in whole mouse islets – We have previously shown that glucose decreases mitochondrial glutathione oxidation in correlation with the increase in NAD(P)H autofluorescence in β -cells (48), and that both effects result from a progressive reduction of the reverse mode of operation of nicotinamide nucleotide transhydrogenase (42). We therefore tested the effect of glucose and exogenous H₂O₂ on NAD(P)H autofluorescence and on cytosolic and mitochondrial H₂O₂ in whole islets from transgenic mice expressing mt-roGFP2-Orp1 or roGFP2-Orp1 globally (*ROSA26/CAG-stop^{fl}-(mito-)roGFP2-Orp1* × *CMV-Cre*)(12). Figure 5 shows that the stimulation with glucose reduced the oxidation ratio of mt-roGFP2-Orp1 under control conditions (and tended to do so for roGFP2-Orp1), and that it decreased or delayed the oxidation of the mitochondrial probe by 100 and 500 μ M H₂O₂ and the oxidation of the cytosolic probe by 500 μ M H₂O₂. These changes in (mt-)roGFP2-Orp1 oxidation were preceded by opposite changes in NAD(P)H autofluorescence in the same islets, confirming the link between both parameters.

Glucose concentration-response curve and effect of MMS, Leu/Gln and KIC on (mt-)roGFP2-Orp1 fluorescence ratio in rat islet cells – We next compared the effect of increasing glucose concentrations and several nutrients that stimulate mitochondrial metabolism, i.e. 20mM monomethylsuccinate (MMS), 10mM α -ketoisocaproate (KIC), and a combination of 10mM leucine and 10mM glutamine (Leu/Gln), on insulin secretion, mt-roGFP2-Orp1 oxidation under control conditions, and the oxidation of both mitochondrial and cytosolic probes by 15 μ M exogenous H₂O₂. The rationale of the latter protocol was to increase the sensitivity of the cytosolic probe to small changes in H₂O₂ concentration by increasing its oxidation ratio to 20-30% (26). Figure 6 shows that, while glucose only stimulated insulin secretion above 5mM, its ability to reduce (mt-)roGFP2-Orp1 or to prevent its oxidation by H₂O₂ was maximal at 5mM in the cytosol and semi-maximal and maximal at 5 and 10mM in the mitochondrial matrix. Among the other nutrients tested, MMS was less potent than Leu/Gln or KIC to stimulate insulin secretion at 0.5 or 5mM glucose (Fig. 6A). These insulin secretagogues also reduced mt-roGFP2-Orp1 under control conditions (Fig. 6B-C) and protected both probes from oxidation by 15 μ M H₂O₂ (Fig. 6D-F), but the amplitude of these effects was not correlated with that on insulin secretion in the absence of exogenous H₂O₂. In the mitochondrial matrix, Leu/Gln was less effective than MMS and KIC, and the effect was smaller than that of G10 alone (Fig. 6C). Similar results were observed in the presence of exogenous H₂O₂, except for the effect of KIC, which was stronger than that of G10 and G30 alone (Fig. 6F). In the cytosol, MMS and Leu/Gln were also less potent, and KIC was more potent, than G10 alone (Fig. 6E). In the presence of exogenous H₂O₂, the stronger protective effect of KIC on the cytosolic probe may have resulted from the capacity of α -ketoacids to degrade H₂O₂ non-enzymatically (32). In agreement with that hypothesis, this effect of KIC was almost identical to that of H₂O₂ removal (compare Fig. 2D with Fig. 6D).

Low concentrations of exogenous H₂O₂ and menadione do not stimulate insulin secretion – To further evaluate the potential role of H₂O₂ as a metabolic coupling factor in GSIS, we tested the effect of very low concentrations of H₂O₂, around the limit of detection by (mt-)roGFP2-Orp1, on [Ca²⁺]_i and GSIS. Table 2 shows that, even at these low concentrations, H₂O₂ was not degraded significantly during 1h incubation at 37°C. Nevertheless, addition of 1-15 μ M exogenous H₂O₂ did not significantly alter [Ca²⁺]_c and insulin secretion at non-stimulating glucose concentrations (Fig. 7AB and DE), nor did it alter the stimulation of insulin secretion by high potassium-induced depolarization at any glucose concentration (Fig. 7G) or by MMS, KIC and Leu/Gln (Fig. 7H). Low concentrations of menadione close to the limit of detection by (mt-)roGFP2-Orp1 (Fig. 2J, 2R) slightly increased [Ca²⁺]_c (Fig. 7C) but did not increase insulin secretion at non-stimulating glucose concentrations, and tended to decrease its stimulation by G10 and G20 (Fig. 7F). Finally, expression of roGFP2-Orp1 or mt-roGFP2-Orp1 did not affect GSIS (Fig. 7I).

Discussion

This study demonstrates that glucose and several nutrients (Leu/Gln, MMS and KIC) that stimulate mitochondrial metabolism while bypassing glycolysis decrease the concentration of H₂O₂ in the mitochondrial matrix of rat pancreatic β -cells and help them degrade exogenous H₂O₂ in the cytosol and mitochondrial matrix. This study also provides arguments against a role for a global increase in intracellular H₂O₂ as a metabolic coupling factor in GSIS. This conclusion relies on two sets of observations. First, acute stimulation with glucose did not increase H₂O₂ in the cytosol or mitochondrial matrix of rat pancreatic β -cells, as measured with the H₂O₂-sensitive probe (mt-roGFP2-Orp1 and confirmed with HyPer/SypHer in the cytosol (for the strong pH-dependent effect of glucose on mitochondrial HyPer/SypHer, see (41)). On the contrary, stimulation with glucose and MMS, Leu/Gln or KIC had a net reductive effect on mitochondrial roGFP2-Orp1 under control conditions, and protected the cytosolic and mitochondrial probes against oxidation by low concentrations of exogenous H₂O₂. Second, low concentrations of exogenous H₂O₂, slightly below or above its limit of detection by roGFP2-Orp1 and HyPer/SypHer, did not affect islet insulin secretion, neither at low, intermediate and high glucose concentrations under control or depolarizing conditions, nor in the presence of Leu/Gln, MMS or KIC.

Protective effects of nutrients against H₂O₂ – Glucose, MMS, Leu/Gln and KIC protected both the cytosolic and mitochondrial probes against oxidation by exogenous H₂O₂. Although this experimental protocol does not reproduce the gradients in H₂O₂ concentration between subcellular compartments that likely occur upon stimulation with nutrients, it was required to detect an effect of glucose on cytosolic roGFP2-Orp1 oxidation. A possible explanation for this requirement is that the moderate oxidation of the probe increased its sensitivity to low changes in H₂O₂ concentration (as explained in figure 6 of (26)). Alternatively, another factor varying with glucose, Leu/Gln and MMS, e.g. NADPH, could exert its action on probe oxidation only if it was first oxidized. In both cases, our observation showing that the nutrients tested were similarly potent against mt-roGFP2-Orp1 in the absence and presence of exogenous H₂O₂ suggests that the results obtained under the latter condition in the cytosol are relevant to β -cell physiology.

The strong protective effect of KIC against exogenous H₂O₂ most likely resulted from the spontaneous stoichiometric reaction of α -ketoacids with H₂O₂ (32), confounding the impact of KIC metabolism on β -cell H₂O₂. It will not be further discussed here. The effects of glucose occurred over a different range of concentrations in the cytosol and mitochondrial matrix, and did not correlate with the stimulation of insulin secretion. That the protective effect of glucose saturated at 5mM in the cytosol is in good agreement with a recent study showing that cytosolic NADPH increases between 0 and 5mM glucose (5). This supports the idea that the rise in NADPH plays a major role in

β -cell antioxidant defenses. Accordingly, when both NADPH and roGFP2-Orp1 oxidation were recorded simultaneously in the presence of H₂O₂, the latter only increased after NADPH had markedly decreased. The presence of a large effect of MMS and Leu/Gln at 0.5mM but not 5mM glucose also indicates that even if mitochondrial metabolism may participate in the protection of the cytosolic probe against oxidation by H₂O₂, this protection is not larger than that afforded by 5mM glucose, a concentration just below the threshold for the stimulation of insulin secretion. By contrast, the protective effect of glucose in the mitochondrial matrix was observed at glucose concentrations that are relevant for the stimulation of mitochondrial metabolism and ATP production, i.e. from 0 to 10mM glucose, with an additional effect of MMS and Leu/Gln at both 0.5 and 5mM glucose. This protective effect correlated with the reduction of the mitochondrial glutathione redox potential measured with mt-Grx1-roGFP2 (48), an effect related to the rise in mitochondrial NADPH, which depends on the activity of nicotinamide nucleotide transhydrogenase (42). The nutrient-induced changes in mt-roGFP2-Orp1 oxidation therefore likely result from an increase in NADPH that exceeds that of H₂O₂, thereby reducing the probe oxidation or increasing probe reduction by thioredoxin and glutathione-dependent enzymatic antioxidant defenses.

Is H₂O₂ a metabolic coupling factor in GSIS? Considerations on the use of H₂O₂-sensitive probes -

Our observation that low concentrations of H₂O₂ do not alter basal insulin secretion and its stimulation by glucose, MMS, Leu/Gln or KIC, is in agreement with previous studies showing that the increased expression of antioxidant enzymes in the mitochondrial matrix, the cytosol or the endoplasmic reticulum of insulin-secreting β -cells does not alter acute GSIS despite effective protection against oxidative stress (6,21,25). Our inability to detect a rise in H₂O₂ upon stimulation with glucose also corroborates previous studies showing that the oxidation of dihydrodichlorofluorescein and dihydroethidine was higher in β -cells acutely exposed to low rather than high glucose concentrations (24,38,43). It is also in keeping with our recent studies showing that glucose, MMS and Leu/Gln acutely reduce the oxidation of mitochondrial roGFP1 and Grx1-roGFP2, which respectively sense thiol and glutathione oxidation, in rat β -cells (41,48). Our results, however, markedly contrast with some reports suggesting that stimulation with glucose acutely increases β -cell reactive oxygen species and that this increase is involved in GSIS (4,11,18,33). The reason for the discrepancy between studies using the same fluorescent probes (dihydrodichlorofluorescein and dihydroethidine) is not clear, but may include differences between insulin-secreting cell lines, whole islets and purified β -cells, and experimental details.

The discrepancy between our results and a recent study using HyPer in INS1 cells and whole rat islets (30) is also obscure. In that study, a small increase in (mt-)HyPer fluorescence ratio upon stimulation with glucose resulted from a rise in H₂O₂ from 20 to 50nM that was unaffected when the glucose-induced pH changes (measured with SNARF-1) were markedly reduced by 20mM HEPES, and that

was suppressed by (mito)catalase overexpression and SOD2 knockdown. In our study, HyPer and SypHer traces were almost identical upon glucose changes, both in the absence and presence of 20mM HEPES (see Fig. 4B and E). In addition, overexpression of SOD1 and SOD2 did not reveal a glucose effect on the cytosolic roGFP2-Orp1 fluorescence ratio, although this probe was more sensitive to low concentrations of exogenous H₂O₂ than HyPer when tested in whole islets under similar conditions (compare figures 2E and 4A and D). We also exclude the hypothesis that our inability to detect a rise in H₂O₂ upon stimulation with glucose resulted from the antioxidant action of the probes themselves, as it has been shown that such an effect is negligible (2,28,40) (Please note that, for a reader who remains convinced that the (mt-)roGFP2-Orp1 probes act as antioxidants in cells, the lack of impact of probe expression on GSIS would reinforce the conclusion that low levels of H₂O₂ do not play a role in GSIS).

Whatever the reason why we and Neal et al obtained contradictory results, we clearly showed that the HyPer fluorescence ratio reports subtle changes in cytosolic pH upon stimulation with glucose, even in the presence of 20mM HEPES. We therefore insist that, in the cytosol as well as in the mitochondrial matrix (41), SypHer should be used in parallel with HyPer to check the effect of pH changes. Although we did not test it, the conclusion should remain valid for the new versions of HyPer which were not designed to be less pH-sensitive than the original probe we used (3,23).

Despite its higher sensitivity to H₂O₂, roGFP2-Orp1 only reacted to 2 to 5μM exogenous H₂O₂ in the cytosol and to 10-20μM H₂O₂ in the mitochondrial matrix. According to (45), and by analogy with the difference in HyPer sensitivity to H₂O₂ between permeabilized and intact INS1 cells (30), this could match a sensitivity to about 100-times lower intracellular H₂O₂ concentrations, in the middle to upper range of signaling H₂O₂ concentrations (1-100nM). We can therefore not exclude that small changes in H₂O₂ may have escaped detection, because they were too local to be detected with whole cell imaging, they were too low to be detected by the probe, or they reacted faster with peroxiredoxins while possibly exerting a signaling role (46,47). Testing these possibilities will require using roGFP2-Orp1 or HyPer/SypHer targeted to specific areas of the cytosol, e.g. at exocytosis sites near the plasma membrane or mitochondria, or using the more sensitive 2-Cys peroxiredoxin-based H₂O₂ sensor roGFP2-Tsa2ΔC_R when it is adapted to mammalian cells (28,40). Superoxide anions could also be involved in GSIS in the absence of a detectable increase in H₂O₂, as SODs are typically expressed at low levels in pancreatic β-cells. However, despite its ability to slightly increase [Ca²⁺]_i and to oxidize both cytosolic and mitochondrial roGFP2-Orp1, menadione, which produces superoxide mainly in the mitochondria, did not stimulate insulin secretion at non-stimulating glucose concentration and did decrease its stimulation by glucose.

In conclusion, we have shown that glucose, MMS, Leu/Gln and KIC acutely decrease the concentration of H₂O₂ in the mitochondrial matrix of rat pancreatic β-cells and help them degrade

exogenous H₂O₂ in the cytosol and mitochondrial matrix. We have also shown that low concentrations of H₂O₂ and menadione do not affect basal and nutrient-induced insulin secretion, thereby providing solid evidence against the putative role of a rise in H₂O₂ in the GSIS by rat pancreatic β -cells.

Innovation (max 100 words)

Whether a rise in H₂O₂ plays a role in the glucose-dependent stimulation of insulin secretion by pancreatic β -cells is highly controversial. Using cytosolic and mitochondrial roGFP2-Orp1 and HyPer, together with the related SypHer pH-probe, we provide strong evidence that nutrients favor H₂O₂ degradation in both compartments, and that low concentrations of H₂O₂ and menadione do not stimulate insulin secretion. Nevertheless, a very small localized rise in H₂O₂ may still play a role in GSIS. The paper also demonstrates that measuring H₂O₂ with HyPer is only valid if controlled with SypHer, even if the expected pH changes seem negligible.

Material and Methods

Chemicals - Glucose was from Merck (Darmstadt, Germany, catalog # 108342). Salts (NaCl, KCl, CaCl₂ and MgCl₂) and NaHCO₃ contained in Krebs solutions (KRB) were from VWR (Radnor, Pennsylvania, USA, catalog # 27810.295, 26764.298, 22317.297, 25108.295 and 27778.293). H₂O₂ (catalog # H1009), menadione (catalog # M5625), dithiothreitol (DTT, catalog # D0632), aldrithiol (AT2, catalog # 143049), monomethylsuccinate (catalog # 81101), leucine (catalog # L8000), glutamine (catalog # 49419), and α -ketoisocaproate (catalog # K0629) were from Sigma (Saint-Louis, Missouri, USA). Each week, the absorbance of the H₂O₂ stock solution was measured at λ 240 nm to compensate for its slow degradation (31). Final dilutions of H₂O₂ in KRB were prepared just before exposing the islets.

Adenoviruses - The generation of an adenovirus encoding the red fluorescent protein DsRed under the control of the rat insulin promoter (RIP-DsRed) was described previously (37). Adenoviruses coding roGFP2-Orp1, mt-roGFP2-Orp1 and HyPer under the control of the CMV promoter were generated and amplified using the AdEasy System (22). The cDNA coding mt-roGFP2-Orp1 was created by inserting the mitochondrial targeting sequence of ATP synthase subunit 9 from *Neurospora Crassa* in N-terminal position of the cDNA coding roGFP2-Orp1 between XhoI and BamHI restriction sites. For each probe, the coding cDNA was inserted in the pShuttle-CMV vector and recloned in the adenoviral backbone plasmid pAdEasy. The resulting plasmids and the pAd-SypHer (a gift from Andreas Wiederkehr from the Nestlé Institute of Health Sciences, Lausanne, Switzerland) were transfected into human embryonic kidney (HEK)-293 cells to generate adenovirus particles. All adenoviruses were amplified in HEK-293 cells, purified on CsCl gradient and quantified using the Adeno-X Rapid Titer Kit (Clontech, Mountain View, California, USA, catalog # 632250). The

adenoviruses encoding catalase, mt-catalase, SOD1 and SOD2 under the control of the CMV promoter (Ad-Cat, Ad-mt-Cat, Ad-SOD1, Ad-SOD2) were obtained from Beverly L. Davidson and John Engelhardt (Gene Transfer Vector Core, University of Iowa, Iowa City, IA, U.S.A.). The empty adenovirus (Ad-Null) was provided by Mark Van de Casteele (Vrije Universiteit Brussel, Brussels, Belgium).

Islet isolation, dispersion and culture - All experiments were approved by the local ethics committee for animal experimentation (Projects 2013/UCL/MD/016, 2017/UCL/MD/014 and DKFZ/213). Islets from male Wistar rats (~8 to 10-week-old, body weight ~200-220g) were isolated by collagenase (Roche, Basel, Switzerland, catalog # 11213873001) digestion of their pancreas, followed by density gradient centrifugation using Histopaque 1077 (Sigma, catalog # 10771) as described (17). After washing and hand-picking the islets under a stereomicroscope to ensure high purity of the preparation, they were cultured at 37°C and 5% CO₂ in serum-free RPMI 1640 medium (Thermo Fisher Scientific, Waltham, Massachusetts, USA, catalog # 31870-025), supplemented with 5g/l BSA fraction V (Roche, catalog # 107351080001), 2mM glutamine, 100units/ml penicillin (Thermo Fisher Scientific, catalog # 15140-122) and 100µg/ml streptomycin (Thermo Fisher Scientific, catalog # 15290-026). In some experiments, islets were dispersed in clusters using trypsin (Thermo Fisher Scientific, catalog # 25200-072) and gentle pipetting in a Ca²⁺-free medium. These clusters were plated on glass coverslips and cultured at 37°C and 5% CO₂ in an RPMI 1640 medium supplemented with 10% FBS, 2mM glutamine, 100units/ml penicillin and 100µg/ml streptomycin.

Adenoviral infection - Cells clusters and islets were infected by adenoviruses encoding RIP-DsRed, roGFP2-Orp1, mt-roGFP2-Orp1 or HyPer/SypHer with a multiplicity of infection of about 15 for the clusters and about 100 for the islets. They were then cultured for 2-3 days before fluorescence measurements.

Immunodetection of antioxidant enzymes - Cell clusters were infected by Ad-Cat, Ad-mt-Cat, Ad-SOD1 and Ad-SOD2, or Ad-null as control, with a multiplicity of infection of 10 for Ad-mt-Cat and 25 for Ad-Cat, Ad-SOD1 and Ad-SOD2. Two days later, the clusters were incubated for 15min with 200nM MitoTracker Red CMXRos (Thermo Fisher Scientific, catalog # M7512), fixed in 4% paraformaldehyde, permeabilized with ice-cold methanol and then incubated overnight with mouse anti-catalase (Sigma, catalog # C0979), rabbit anti-SOD1 or rabbit anti-SOD2 (Abcam, Cambridge, UK, catalog # ab16831 and ab13533) antibody diluted 1:200. On the second day, the coverslips were washed in Phosphate-buffered saline and incubated for two hours with Alexa Fluor Green 488-conjugated goat anti-mouse or anti-rabbit antibodies (Thermo Fischer Scientific, catalogue # A11017 and # A11070). The red and green fluorescence intensities were measured by epifluorescence microscopy with a x20 objective and their localization was analyzed by confocal microscopy.

Confocal microscopy - The fluorescence of islet cell clusters or islets expressing (mt-)roGFP2-Orp1,

HyPer or SypHer and labelled with the mitochondrial stain MitoTracker Red CMXRos or expressing DsRed was analyzed at room temperature using a confocal microscope (Nikon Eclipse TE2000-E equipped with a Yokogawa CSU-10 spinning disk from Visitech International) with a x100 objective. For (mt-)roGFP2-Orp1, HyPer and SypHer, cells were excited at 491nm with an emission filter of 503-552nm. For DsRed and MitoTracker Red, cells were excited at 561nm with an emission filter of 630-690nm. To allow superposition, monochrome images were converted in green or red images using ImageJ software.

Dynamic measurements of (mt-)roGFP2-Orp1 and HyPer/SypHer fluorescence ratio - After culture, the coverslip coated with cell clusters was mounted in a chamber maintained at 37°C and placed on the stage of an inverted microscope equipped with a x40 objective. Entire islets were transferred in the chamber and analyzed through a x20 objective. Cell clusters or islets were perfused at a flow rate of 1ml/min with a bicarbonate-buffered Krebs solution (KRB) containing 120mM NaCl, 4.8mM KCl, 2.5mM CaCl₂, 1.2mM MgCl₂, 24mM NaHCO₃, 1g/l BSA, and various glucose concentrations, other nutrients and low concentrations of freshly added exogenous H₂O₂. This solution was continuously gazed with O₂/CO₂ (94/6) to maintain a pH of around 7.4. The fluorescence ratio of (mt-)roGFP2-Orp1 and HyPer/SypHer was measured every 30 seconds after double excitation, at 400/480nm or 480/400nm respectively, and emission at 535nm. To allow comparison between the various experiments, (mt-)roGFP2-Orp1 fluorescence ratios were normalized to the ratio of the maximally-reduced probe, set to 0%, and that of the maximally-oxidized probe, set to 100%, as measured at the end of each experiment after addition of 10mM DTT followed by 100μM AT2. Cytosolic HyPer/SypHer fluorescence ratios were normalized to the initial ratio at 10mM glucose (set to 0%) and the peak ratio measured after addition of 30mM NH₄Cl (set to 100%). Because single cells and small clusters of 2-4 cells were more sensitive to H₂O₂ than larger ones, the fluorescence ratio of the probes was only analyzed in clusters of at least 5 cells or in whole islets.

Dynamic recordings of changes in cytosolic Ca²⁺ concentration - After culture, islet cell clusters were loaded for two hours with 2μM fura-2 LR acetoxymethyl ester (catalog # 0108, TEF Labs, Austin, Texas) and the probe fluorescence ratio (λ_{ex} 340/380nm; λ_{em} 510nm), recorded every five seconds during perfusion, was used as an indicator of the free cytosolic Ca²⁺ concentration ([Ca²⁺]_c) (17).

Simultaneous recording of the NAD(P)H autofluorescence and (mt-)roGFP2-Orp1 oxidation ratio in whole mouse islets - Changes in NAD(P)H and roGFP2-Orp1 fluorescence were simultaneously recorded in incubated islets using a microplate reader (Pherastar FS microplate reader, BMG-Labtech, Ortenberg, Germany). Islets were isolated from 4-to-6 month-old male transgenic mice expressing cytosolic or mitochondrial roGFP2-ORP1 (*ROSA26/CAG-stop^{fl}-(mito-)roGFP2-Orp1 × CMV-Cre*) or from control non-fluorescent mice with intact stop cassette (12). After isolation, islets were cultured overnight in standard RPMI medium supplemented with 10% FBS. Before the experiment,

islets were collected, rinsed in KRB containing 2mM glucose and 0.1% BSA for 10 min, and transferred to a U-shaped 96-well plate (TPP Cat #92097), at 20-25 islets per well in a total volume of 160µl. Controls of maximum oxidation (diamide 2mM) and reduction (DTT 10mM) were also included. The islets were then centrifuged at 200xg for 3min and NAD(P)H autofluorescence (λ_{ex} 340nm, λ_{em} 460nm) and roGFP2 fluorescence (λ_{ex} 405/488nm, λ_{em} 520nm) were measured at 37°C. After 9 complete cycles (about 1min each), 20µl of glucose (final concentration in low glucose: 2mM; high glucose: 20mM) and 20µl of H₂O₂ (final concentration: 100µM or 500µM) were added to the well and incubation was continued at 37°C for 90-170min. At the end of experiment, OxD was calculated as described (27).

Insulin secretion - After culture in serum-free RPMI 1640 medium supplemented with 5g/l BSA, islets were incubated for 40min in KRB containing 0.5mM glucose. Batches of 5 islets were then incubated for one hour under various experimental conditions. After incubation, insulin was measured in the medium by in-house RIA using rat insulin as standard, I¹²⁵-labelled porcine insulin as tracer, and a specific anti-insulin guinea-pig serum (14). The insulin and DNA content of islets was measured by RIA and SYBR Green fluorimetry.

Statistical analysis: Results are shown as means \pm SEM for the number of observations indicated in the figure legends. The statistical significance of differences between groups was assessed as detailed in the figure legends. For each type of comparison, the degree of significance is indicated by a letter (a-d; e-h; m-p) corresponding to the same *P* value throughout the paper, i.e. *a*, *e* and *m* for *P*<0.05; *b*, *f* and *n* for *P*<0.01; *c*, *g* and *o* for *P*<0.001; *d*, *h* and *p* for *P*<0.0001.

Acknowledgments

We thank Dr Andreas Wiederkehr (Nestlé Institute of Health Sciences, Lausanne, Switzerland) for providing Ad-SypHer and Ad-*mt*-SypHer. We thank Vinciane El-Hawat and Morgane Wéry for their contribution as Master's students, and Céline Bricteux and Fabien Knockaert for expert technical help.

Funding

JCJ and PG are Research Directors at the Fonds de la Recherche Scientifique-FNRS, Brussels, Belgium. This study was funded by the Action de Recherche Concertée 12/17-047 from the Communauté française de Belgique, the "Fonds Spécial de Recherche 2016" from the Université catholique de Louvain, and Grant no. SFD/MSD 2016 from the Société Francophone du Diabète (Paris, France) to JCJ. LPR was supported by DKFZ Visiting Scientist Program. TPD acknowledges funding by the DFG (SFB1036 and SPP1710).

Author's contributions

JPD, LPR and JCJ conceived and designed the experiments. JPD, LPR, DPF and JCJ performed the experiments and analyzed the data. TPD designed and generated R26/mito-roGFP2-Orp1 mice and discussed the results and protocols. PG contributed to confocal microscopy and supplied Ad-RIP-DsRed. JPD, LPR and JCJ wrote the paper. All other co-authors edited and approved the paper.

Author Disclosure Statement

No competing financial interests exist for JPD, LPR, DPF, PG, TPD and JCJ.

References

1. Belousov VV, Fradkov AF, Lukyanov KA, Staroverov DB, Shakhbazov KS, Terskikh AV, Lukyanov S. Genetically encoded fluorescent indicator for intracellular hydrogen peroxide. *Nat Methods* 3: 281-286, 2006.
2. Bilan DS, Belousov VV. New tools for redox biology: From imaging to manipulation. *Free Rad Biol Med* 109: 167-188, 2017.
3. Bilan DS, Pase L, Joosen L, Gorokhovatsky AY, Ermakova YG, Gadella TW, Grabher C, Schultz C, Lukyanov S, Belousov VV. HyPer-3: a genetically encoded H₂O₂ probe with improved performance for ratiometric and fluorescence lifetime imaging. *ACS Chem Biol* 8: 535-542, 2013.
4. Bindokas VP, Kuznetsov A, Sreenan S, Polonsky KS, Roe MW, Philipson LH. Visualizing superoxide production in normal and diabetic rat islets of Langerhans. *J Biol Chem* 278: 9796-9801, 2003.
5. Cameron WD, Bui CV, Hutchinson A, Loppnau P, Graslund S, Rocheleau JV. Apollo-NADP⁺: a spectrally tunable family of genetically encoded sensors for NADP⁺. *Nat Methods* 13: 352-358, 2016.
6. Chen J, Saxena G, Mungrue IN, Lusic AJ, Shalev A. Thioredoxin-interacting protein: a critical link between glucose toxicity and β -cell apoptosis. *Diabetes* 57: 938-944, 2008.
7. Chuang YY, Chen Y, Gadisetti, Chandramouli VR, Cook JA, Coffin D, Tsai MH, DeGraff W, Yan H, Zhao S, Russo A, Liu ET, Mitchell JB. Gene expression after treatment with hydrogen peroxide, menadione, or t-butyl hydroperoxide in breast cancer cells. *Cancer Res* 62: 6246-6254, 2002.
8. de Souza AH, Santos LR, Roma LP, Bensellam M, Carpinelli AR, Jonas JC. NADPH oxidase-2 does not contribute to beta-cell glucotoxicity in cultured pancreatic islets from C57BL/6J mice. *Mol Cell Endocrinol* 439: 354-362, 2017.
9. Elsner M, Gehrmann W, Lenzen S. Peroxisome-generated hydrogen peroxide as important mediator of lipotoxicity in insulin-producing cells. *Diabetes* 60: 200-208, 2011.
10. Ferdaoussi M, Dai X, Jensen MV, Wang R, Peterson BS, Huang C, Ilkayeva O, Smith N, Miller N, Hajmrle C, Spigelman AF, Wright RC, Plummer G, Suzuki K, Mackay JP, van de Bunt M, Gloyn AL, Ryan TE, Norquay LD, Brosnan MJ, Trimmer JK, Rolph TP, Kibbey RG, Manning Fox JE, Colmers WF, Shirihai OS, Neuffer PD, Yeh ET, Newgard CB, MacDonald PE. Isocitrate-to-SEN1 signaling amplifies insulin secretion and rescues dysfunctional beta cells. *J Clin Invest* 125: 3847-3860, 2015.

11. Fu J, Zhang Q, Woods CG, Zheng H, Yang B, Qu W, Andersen ME, Pi J. Divergent effects of sulforaphane on basal and glucose-stimulated insulin secretion in beta-cells: role of reactive oxygen species and induction of endogenous antioxidants. *Pharm Res* 30: 2248-2259, 2013.
12. Fujikawa Y, Roma LP, Sobotta MC, Rose AJ, Diaz MB, Locatelli G, Breckwoldt MO, Misgeld T, Kerschensteiner M, Herzig S, Muller-Decker K, Dick TP. Mouse redox histology using genetically encoded probes. *Sci Signal* 9 (419): rs1, 2016.
13. Hedekov CJ, Capito K, Thams P. Cytosolic ratios of free [NADPH]/[NADP⁺] and [NADH]/[NAD⁺] in mouse pancreatic islets, and nutrient-induced insulin secretion. *Biochem J* 241: 161-167, 1987.
14. Heding LG. Determination of total serum insulin (IRI) in insulin-treated diabetic patients. *Diabetologia* 8: 260-266, 1972.
15. Ivarsson R, Quintens R, Dejonghe S, Tsukamoto K, In't Veld PA, Renstrom E, Schuit FC. Redox control of exocytosis: regulatory role of NADPH, thioredoxin, and glutaredoxin. *Diabetes* 54: 2132-2142, 2005.
16. Khaldi MZ, Elouil H, Guiot Y, Henquin JC, Jonas JC. The antioxidants N-acetyl-L-cysteine and manganese(III)tetrakis (4-benzoic acid)porphyrin do not prevent β -cell dysfunction in rat islets cultured in high glucose for 1 wk. *Am J Physiol Endocrinol Metab* 291: E137-E146, 2006.
17. Khaldi MZ, Guiot Y, Gilon P, Henquin JC, Jonas JC. Increased glucose sensitivity of both triggering and amplifying pathways of insulin secretion in rat islets cultured for one week in high glucose. *Am J Physiol Endocrinol Metab* 287: E207-E217, 2004.
18. Leloup C, Tourrel-Cuzin C, Magnan C, Karaca M, Castel J, Carneiro L, Colombani AL, Ktorza A, Casteilla L, Penicaud L. Mitochondrial reactive oxygen species are obligatory signals for glucose-induced insulin secretion. *Diabetes* 58: 673-681, 2009.
19. Lenzen S. Chemistry and biology of reactive species with special reference to the antioxidative defence status in pancreatic beta-cells. *Biochim Biophys Acta* 1861: 1929-1942, 2017.
20. Li N, Li B, Brun T, Deffert-Delbouille C, Mahiout Z, Daali Y, Ma XJ, Krause KH, Maechler P. NADPH oxidase NOX2 defines a new antagonistic role for reactive oxygen species and cAMP/PKA in the regulation of insulin secretion. *Diabetes* 61: 2842-2850, 2012.
21. Lortz S, Gurgul-Convey E, Naujok O, Lenzen S. Overexpression of the antioxidant enzyme catalase does not interfere with the glucose responsiveness of insulin-secreting INS-1E cells and rat islets. *Diabetologia* 56: 774-782, 2013.
22. Luo J, Deng ZL, Luo X, Tang N, Song WX, Chen J, Sharff KA, Luu HH, Haydon RC, Kinzler KW, Vogelstein B, He TC. A protocol for rapid generation of recombinant adenoviruses using the AdEasy system. *Nat Protoc* 2: 1236-1247, 2007.
23. Markvicheva KN, Bilan DS, Mishina NM, Gorokhovatsky AY, Vinokurov LM, Lukyanov S, Belousov VV. A genetically encoded sensor for H₂O₂ with expanded dynamic range. *Bioorg Med Chem* 19: 1079-1084, 2011.
24. Martens GA, Cai Y, Hinke S, Stange G, Van de Castele M, Pipeleers D. Glucose suppresses superoxide generation in metabolically responsive pancreatic β cells. *J Biol Chem* 280: 20389-20396, 2005.
25. Mehmeti I, Lortz S, Elsner M, Lenzen S. Peroxiredoxin 4 improves insulin biosynthesis and glucose-induced insulin secretion in insulin-secreting INS-1E cells. *J Biol Chem* 289: 26904-13, 2014.
26. Meyer AJ, Dick TP. Fluorescent protein-based redox probes. *Antioxid Redox Signal* 13: 621-650, 2010.
27. Morgan B, Sobotta MC, Dick TP. Measuring E GSH and H₂O₂ with roGFP2-based redox probes. *Free Radic Biol Med* 51: 1943-1951, 2011.

28. Morgan B, Van Laer K, Owusu TN, Ezerina D, Pastor-Flores D, Amponsah PS, Tursch A, Dick TP. Real-time monitoring of basal H₂O₂ levels with peroxiredoxin-based probes. *Nat Chem Biol* 12: 437-43, 2016.
29. Muller A, Schneider JF, Degrossoli A, Lupilova N, Dick TP, Leichert LI. Systematic in vitro assessment of responses of roGFP2-based probes to physiologically relevant oxidant species. *Free Radic. Biol Med* 106: 329-338, 2017.
30. Neal A, Rountree A, Kernan K, Van YB, Zhang H, Reed BJ, Osborne W, Wang W, Sweet IR. Real-time imaging of intracellular hydrogen peroxide in pancreatic islets. *Biochem J* 473: 4443-4456, 2016.
31. Noble RW, Gibson QH. The reaction of ferrous horseradish peroxidase with hydrogen peroxide. *J Biol Chem* 245: 2409-2413, 1970.
32. O'Donnell-Tormey J, Nathan CF, Lanks K, DeBoer CJ, de la Harpe J. Secretion of pyruvate. An antioxidant defense of mammalian cells. *J Exp Med* 165: 500-514, 1987.
33. Pi J, Bai Y, Zhang Q, Wong V, Floering LM, Daniel K, Reece JM, Deeney JT, Andersen ME, Corkey BE, Collins S. Reactive oxygen species as a signal in glucose-stimulated insulin secretion. *Diabetes* 56: 1783-1791, 2007.
34. Pi J, Zhang Q, Fu J, Woods CG, Hou Y, Corkey BE, Collins S, Andersen ME. ROS signaling, oxidative stress and Nrf2 in pancreatic beta-cell function. *Toxicol Appl Pharmacol* 244: 77-83, 2009.
35. Poburko D, Santo-Domingo J, Demaurex N. Dynamic regulation of the mitochondrial proton gradient during cytosolic calcium elevations. *J Biol Chem* 286: 11672-11684, 2011.
36. Prentki M, Matschinsky FM, Madiraju SR. Metabolic signaling in fuel-induced insulin secretion. *Cell Metab* 18: 162-185, 2013.
37. Quiox N, Cheng-Xue R, Mattart L, Zeinoun Z, Guiot Y, Beauvois MC, Henquin JC, Gilon P. Glucose and pharmacological modulators of ATP-sensitive K⁺ channels control [Ca²⁺]_c by different mechanisms in isolated mouse α -cells. *Diabetes* 58: 412-421, 2009.
38. Rebelato E, Abdulkader F, Curi R, Carpinelli AR. Control of the intracellular redox state by glucose participates in the insulin secretion mechanism. *PLoS ONE* 6: e24507, 2011.
39. Reinbothe TM, Ivarsson R, Li DQ, Niazi O, Jing X, Zhang E, Stenson L, Bryborn U, Renstrom E. Glutaredoxin-1 mediates NADPH-dependent stimulation of calcium-dependent insulin secretion. *Mol Endocrinol* 23: 893-900, 2009.
40. Roma LP, Deponte M, Riemer J, Morgan B. Mechanisms and Applications of Redox-Sensitive Green Fluorescent Protein-Based Hydrogen Peroxide Probes. *Antioxid Redox Signal*, 2018.
41. Roma LP, Duprez J, Takahashi HK, Gilon P, Wiederkehr A, Jonas JC. Dynamic measurements of mitochondrial hydrogen peroxide concentration and glutathione redox state in rat pancreatic β -cells using ratiometric fluorescent proteins: confounding effects of pH with HyPer but not roGFP1. *Biochem J* 441: 971-978, 2012.
42. Santos LRB, Muller C, de Souza AH, Takahashi HK, Spéjel P, Sweet IR, Chae H, Mulder H, Jonas J-C. NNT reverse mode of operation mediates glucose control of mitochondrial NADPH and glutathione redox state in mouse pancreatic β -cells. *Mol Metab* 6: 535-547, 2017.
43. Sarre A, Gabrielli J, Vial G, Leverve XM, Assimacopoulos-Jeannet F. Reactive oxygen species are produced at low glucose and contribute to the activation of AMPK in insulin-secreting cells. *Free Radic Biol Med* 52: 142-150, 2012.
44. Shepherd RM, Henquin JC. The role of metabolism, cytoplasmic Ca²⁺, and pH-regulating exchangers in glucose-induced rise of cytoplasmic pH in normal mouse pancreatic islets. *J Biol Chem* 270: 7915-7921, 1995.
45. Sies H. Hydrogen peroxide as a central redox signaling molecule in physiological oxidative stress: Oxidative eustress. *Redox Biol* 11: 613-619, 2017.

46. Sobotta MC, Liou W, Stocker S, Talwar D, Oehler M, Ruppert T, Scharf AN, Dick TP. Peroxiredoxin-2 and STAT3 form a redox relay for H₂O₂ signaling. *Nat Chem Biol* 11: 64-70, 2015.
47. Stocker S, Van Laer K, Mijuskovic A, Dick TP. The Conundrum of Hydrogen Peroxide Signaling and the Emerging Role of Peroxiredoxins as Redox Relay Hubs. *Antioxid Redox Signal* 28: 558-573, 2018.
48. Takahashi HK, Santos LR, Roma LP, Duprez J, Broca C, Wojtusciszyn A, Jonas JC. Acute nutrient regulation of the mitochondrial glutathione redox state in pancreatic beta-cells. *Biochem J* 460: 411-423, 2014.
49. Wiederkehr A, Park KS, Dupont O, Demaurex N, Pozzan T, Cline GW, Wollheim CB. Matrix alkalinization: a novel mitochondrial signal for sustained pancreatic β -cell activation. *EMBO J* 28: 417-428, 2009.
50. Wiederkehr A, Wollheim CB. Mitochondrial signals drive insulin secretion in the pancreatic beta-cell. *Mol Cell Endocrinol* 353: 128-137, 2012.

Table 1: Expression of the redox fluorescent probes in pancreatic islet cells**A**

Probe	DsRed-pos	Probe-pos	Coexpression	Fluo-pos	Fluo-neg	Total
roGFP2-Orp1	538 (90%)	582 (97%)	520 (87%)	600	116	716
mt-roGFP2-Orp1	585 (82%)	709 (99%)	583 (82%)	711	94	805
HyPer	791 (73%)	1012 (93%)	714 (66%)	1089	ND	ND
SypHer	752 (70%)	1004 (94%)	689 (65%)	1067	ND	ND

B

Probe	DsRed-pos/Probe-pos (%)	Probe-pos/DsRed-pos (%)	Probe-pos/DsRed-neg (%)
roGFP2-Orp1	520/582 (89.3)	520/538 (96.7)	62/178 (34.8)
mt-roGFP2-Orp1	583/709 (82.2)	583/585 (99.7)	126/220 (57.3)
HyPer	714/1012 (70.6)	714/791 (90.9)	ND
SypHer	689/1004 (65.5)	689/752 (92.4)	ND

A, the number of cells with red (RIP-DsRed) and green (redox probes) fluorescence was counted in the experiments illustrated in figure 1 (three preparations for (mt-)roGFP2-Orp1 and two preparations for HyPer and SypHer). Cells that were negative for both DsRed and probe fluorescence were not detected by confocal microscopy, and the total number of cells was therefore not available for HyPer and SypHer (ND). The proportion of cells relative to the total number of fluorescent-positive (Fluo-pos) cells are shown between brackets. B, the proportion of Ds-Red-positive cells among probe-expressing cells and of probe-expressing cells in DsRed-positive and –negative cells were computed from data shown in panel A.

Table 2: H₂O₂ concentration after 1h incubation

Incubation condition	H₂O₂ (μM)
G0.5 + 1 μM H ₂ O ₂ + islets	1.08 ± 0.22
G0.5 + 4 μM H ₂ O ₂ + islets	4.28 ± 0.69
G0.5 + 15 μM H ₂ O ₂ + islets	14.5 ± 1.20
G10 + 1 μM H ₂ O ₂ + islets	0.9 ± 0.11
G10 + 4 μM H ₂ O ₂ + islets	3.97 ± 0.62
G10 + 15 μM H ₂ O ₂ + islets	13.3 ± 1.15

Batches of 5 islets were pre-incubated for 40 min in G0.5 and incubated for one hour in 1 ml of KRB containing G0.5 or G10 and 1, 4 or 15μM H₂O₂. At the end, H₂O₂ was measured in the supernatants with OxiSelect Hydrogen Peroxide/Peroxidase Assay Kit (Cell BioLabs) using an H₂O₂ standard curve in KRB with no islet. Data are means ± SEM for 3 experiments in duplicates. There was no significant effect of glucose on the concentration of H₂O₂ by 2-way ANOVA + Sidak's multiple comparisons test.

Figure legends

Figure 1: Expression of (mt-)roGFP2-Orp1 and HyPer/SypHer in rat pancreatic islet cells - A-D, rat pancreatic islet cell clusters (A, B) or whole islets (C, D) were co-infected with Ad-roGFP2-Orp1 (A), Ad-mt-roGFP2-Orp1 (B), Ad-HyPer (C) or Ad-SypHer (D) and Ad-RIP-DsRed, and their fluorescence, measured by epifluorescence (A, B) or confocal microscopy (C, D), was converted in green and red pseudo-colors. Nuclei were labelled with Hoechst 33342 (gray level intensities). Shown are representative images from 3 different preparations. E-F, rat islet cell clusters were infected with Ad-roGFP2-Orp1 (E) or Ad-mt-roGFP2-Orp1 (F) and their mitochondria were labelled with 200nM MitoTracker Red. The co-localization of (mt-)roGFP2-Orp1 and mitochondria (confocal microscopy) appears as yellow structures on merged images. Scale bars = 40µm (A and B), 60µm (C and D), 10µm (E and F).

Figure 2: Effects of exogenous H₂O₂, menadione, pH and glucose on (mt-)roGFP2-Orp1 fluorescence ratio - Rat pancreatic islet cell clusters expressing roGFP2-Orp1 (A-J) or mt-roGFP2-Orp1 (K-R) were perfused with KRB containing 5 or 10mM glucose (G5 or G10) and increasing concentrations of H₂O₂ (A-C, K, L), or in KRB containing various glucose concentrations (Gn in mM) alone (F, O, P) or with 5 or 15µM H₂O₂ (G, H). D and M, islet cell clusters were perfused with G10 and exposed to 15µM H₂O₂ for 20min before a 30-min recovery period. I and Q, islet cell clusters were perfused with G10 to which 30mM NaAc and 30mM NH₄Cl were successively added. Rat islets expressing roGFP2-Orp1 (E, J) or mt-roGFP2-Orp1 (N, R) at their periphery were perfused with G10 and increasing concentrations of H₂O₂ (E, N) or menadione (J, R). Data were normalized to the ratios measured in the presence of 10mM DTT (set to 0%) and 100µM AT2 (set to 100%). Results are means ± SEM for 12-49 clusters from 3-6 experiments (A-D, F-I, K-M, O-Q), or for 12 to 18 islets from 3-4 experiments (E, J, N, R). The statistical significance of differences between groups was assessed at each step vs. the initial fluorescence ratio in G10 or G5 by 1-way ANOVA + Dunnett's or by 2-way ANOVA + Tukey's multiple comparisons test (a-d); vs. the previous step by one- or two-way ANOVA + Tukey's multiple comparisons test (e-h); between traces by 2-way ANOVA + Sidak's multiple comparisons test (m-p); *a, e* and *m* for *P*<0.05; *b, f* and *n* for *P*<0.01; *c, g* and *o* for *P*<0.001; *d, h* and *p* for *P*<0.0001.

Figure 3: A-D, Effects of (mito-)catalase, SOD1 and SOD2 overexpression on (mt-)roGFP2-Orp1 responses to H₂O₂ and glucose changes - Rat pancreatic islet cell clusters were co-infected with the adenoviruses coding (mt-)roGFP2-Orp1 and (mito-)catalase or SOD1 and SOD2 under the control of the CMV promoter (Ad-Cat, Ad-MitoCat, Ad-SOD1, Ad-SOD2) or an empty adenovirus as control (Ad-null) at a multiplicity of infection of about 25 (A-B) and 10 (C-D). They were then perfused with KRB containing 10mM glucose (G10) and increasing concentrations of H₂O₂ (C), or in KRB containing

various glucose concentrations (Gn in mM) alone (A, D) or with 15 μ M H₂O₂ (B). Results are means \pm SEM for 16 to 25 clusters from 3 experiments. The statistical significance of differences between groups was assessed at each step vs. the initial fluorescence ratio in G10 by two-way ANOVA + Dunnett's (a-d); vs. the previous step by two-way ANOVA + Tukey's multiple comparisons test (e-h); between traces by two-way ANOVA + Sidak's multiple comparisons test (m-p); *a, e* and *m* for $P < 0.05$; *b, f* and *n* for $P < 0.01$; *c, g* and *o* for $P < 0.001$; *d, h* and *p* for $P < 0.0001$. **E-P, (Over)expression of (mito-)catalase, SOD1 and SOD2 in rat pancreatic islet cells** – Two days after infection with Ad-Cat, Ad-MitoCat, Ad-SOD1, Ad-SOD2, or Ad-null, rat islet cell clusters were loaded with 200nM of Mitotracker Red for 15min, fixed and permeabilized. Catalase, SOD1 and SOD2 were then detected by immunohistochemistry (green fluorescence). E-H, immunodetection of catalase (E, F), SOD1 (G) and SOD2 (H) in cells infected with Ad-null (E-H, left panels) or Ad-Cat, Ad-MitoCat, Ad-SOD1 and Ad-SOD2 (E-H, right panels); epifluorescence microscopy, x20 objective; fixed parameters for Ad-null and Ad-enzyme panels. I-P, the cellular distribution of the antioxidant enzymes was analyzed by confocal microscopy with a x100 objective. The exposure time was optimized for signal detection under each condition; the green fluorescence of Ad-null cells in panels I, K, M may therefore reflect sample autofluorescence. A yellow fluorescence in the merged images indicates mitochondrial expression of the antioxidant enzyme. Representative images from three different preparations are shown. Scale bars = 20 μ m (E-L), 100 μ m (M-P).

Figure 4: Effects of exogenous H₂O₂ and glucose on HyPer and SypHer fluorescence ratios - Rat pancreatic islets expressing untargeted HyPer or SypHer were perfused with KRB containing G10 in the absence (A-C) or presence of 20mM HEPES (D, E) before the addition of increasing H₂O₂ concentrations (A, D) or changes in glucose concentration in the absence (B, E) or presence of 15 μ M H₂O₂ (C). Data were normalized to the initial fluorescence ratio in G10 (set to 0%) and the peak ratio in 30mM NH₄Cl (set to 100%). Note that the scale in B and E markedly enhances the apparent amplitude of the glucose effects. Results are means \pm SEM for 6-15 islets from 3-5 experiments. The statistical significance of differences between groups was assessed at each step vs. the initial fluorescence ratio in G10 by two-way ANOVA + Dunnett's multiple comparisons test (a-d); vs. the previous step by one or two-way ANOVA + Tukey's multiple comparisons test (e-h); between traces by two-way ANOVA + Sidak's multiple comparisons test (m-p); *a, e* and *m* for $P < 0.05$; *b, f* and *n* for $P < 0.01$; *c, g* and *o* for $P < 0.001$; *d, h* and *p* for $P < 0.0001$.

Figure 5: Effects of glucose and exogenous H₂O₂ on NAD(P)H autofluorescence and (mt-)roGFP2-Orp1 OxD. Pancreatic islets from transgenic mice expressing roGFP2-Orp1 (A-F) or mt-roGFP2-Orp1 (A-C, G-I) were incubated with KRB containing 2mM glucose until minute 10 of the recording, then with KRB containing 2 or 20mM glucose (G2 or G20) alone or with 100 or 500 μ M H₂O₂. A-B, NAD(P)H autofluorescence normalized to the average fluorescence level during the initial period in G2. D-E and G-H, oxidation ratios (OxD) of the cytosolic and mitochondrial probes. The normalized NAD(P)H autofluorescence level (C), roGFP2-Orp1 OxD (F) and mt-roGFP2-Orp1 OxD (I) at min 50 (40 min after stimulation) were expressed relative to the level in G2. Results are means \pm SEM for 3 experiments with pooled islets from two mice each. The statistical significance of differences between groups was assessed for the effect of H₂O₂ vs. G2 or G20 alone (a-d) and for the effect of G20 vs. G2 (m-p) by two-way ANOVA + Sidak's multiple comparisons test; *a* and *m* for $P < 0.05$; *b* and *n* for $P < 0.01$; *c* and *o* for $P < 0.001$; *d* and *p* for $P < 0.0001$.

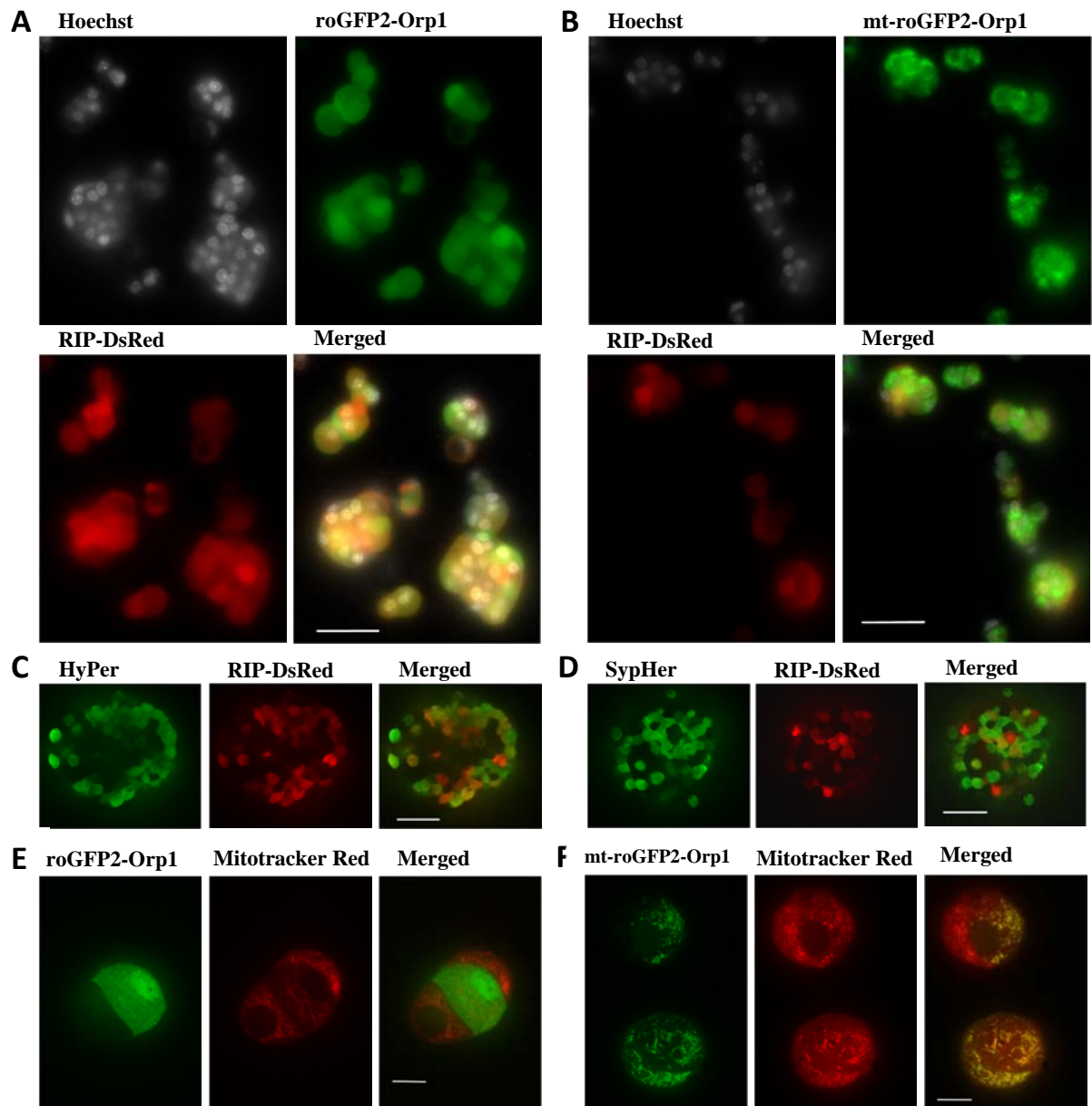
Figure 6: Effects of glucose and other nutrients on insulin secretion and (mt-)roGFP2-Orp1 fluorescence ratio under control condition and in the presence of exogenous H₂O₂ - A, batches of 5 islets were pre-incubated for 40min in KRB containing 0.5mM glucose before one-hour incubation at increasing glucose concentrations, alone or with 20mM monomethylsuccinate (MMS), 10mM Leucine + 10mM Glutamine (Leu/Gln), or 10mM α -ketoisocaproate (KIC), as indicated. Insulin secretion was expressed relative to the islet DNA content. Results are means \pm SEM for 5 experiments in triplicates. The statistical significance of differences between groups was assessed for the effects of G5 vs. G0.5 (a-d) and for the effect of nutrients at the same glucose concentration (e-h) by two-way ANOVA + Sidak's multiple comparisons test; for the effect of G10 vs. G0.5 by one-way ANOVA + Dunnett's multiple comparisons test (m-p); *a* and *e* for $P < 0.05$; *b* and *f* for $P < 0.01$; *c* and *g* for $P < 0.001$; *d* and *h* for $P < 0.0001$.

B-C, islet cell clusters expressing mt-roGFP2-Orp1 were perfused with KRB containing increasing glucose concentrations alone or with MMS, Leu/Gln or KIC as in panel A. B, experimental protocol illustrated with mean traces without error bars for 3 conditions. The fluorescence ratios were normalized as in figure 2. C, the effect of glucose and nutrients was quantified as the mean change in fluorescence ratio from minute 9 to 29 (Δ). D-F, islet cell clusters expressing roGFP2-Orp1 (D and E) or mt-roGFP2-Orp1 (F) were perfused with KRB containing 10 mM glucose and subsequently exposed to 15 μ M H₂O₂. Twenty min later, the islets were exposed to H₂O₂ in the presence of 0.5, 5, 10 or 30mM glucose alone or with MMS, Leu/Gln, or KIC, as indicated. D, illustration of the experimental protocol (mean traces). E and F, efficacy of nutrients against the oxidation of the probe

by H₂O₂ as estimated from the $\Delta 2/\Delta 1$ ratio, where $\Delta 1$ and $\Delta 2$ are the mean change in the fluorescence ratio from minute 9 to 29 ($\Delta 1$) and from minute 29 to 49 ($\Delta 2$) (see panel D). Results are means \pm SEM for 8 to 26 clusters from 3 experiments. The statistical significance of differences between groups was assessed vs. G10 (a-d) or vs. G0.5 or G5 alone (e-h) by one-way Anova + Dunnett's multiple comparisons test; *a* and *e* for $P < 0.05$; *b* and *f* for $P < 0.01$; *c* and *g* for $P < 0.001$; *d* and *h* for $P < 0.0001$.

Figure 7: Effect of low concentrations of exogenous H₂O₂ and menadione on cytosolic Ca²⁺ concentration and insulin secretion. A-D, whole islets were perfused with KRB containing 6mM glucose (G6) and increasing concentrations of H₂O₂ (A,B,D) or menadione (C); fura2-LR fluorescence ratio used as an indicator of changes in cytosolic calcium concentration. A-C, results are means \pm SEM for 11-19 islets from 3-4 experiments. The statistical significance of differences between groups was assessed at each step vs. initial value in G6 (a-d) by one-way Anova + Dunnett's multiple comparisons test; *a* for $P < 0.05$; *b* for $P < 0.01$; *c* for $P < 0.001$; *d* for $P < 0.0001$. D, results are means \pm SEM from 4 perfusions with ~ 100 islets each and are expressed relative to the DNA content. The statistical significance of differences between groups was assessed at each step vs. initial value in G6 (d) by two-way Anova + Dunnett's multiple comparisons test ; *d* for $P < 0.0001$. E-H, batches of 5 islets were pre-incubated for 40min in G0.5 before one-hour incubation at increasing glucose concentrations (G0.5, G2, G6, G10 and G20), alone or with 1 or 4 μ M H₂O₂ (E); alone or with 1, 2 or 5 μ M menadione (F); alone or with 30mM K⁺ (K30) and 0, 4, or 15 μ M H₂O₂ (G); in the absence or presence of different nutrients (MMS, Leu/Gln and KIC), alone or with 15 μ M H₂O₂ (H). Control data in H are the same as in Fig. 6A. I, insulin secretion was measured at increasing glucose concentration 48h after infection with Ad-Null or Ad-(mt-)roGFP2-Orp1 as indicated. Insulin secretion was expressed relative to the islet DNA content. Results are means \pm SEM for 4 experiments in triplicates. The statistical significance of differences between groups was assessed for the effect of glucose vs. G0.5 (a-d) or for the effects of H₂O₂ vs. glucose alone (e-h) by two-way Anova + Dunnett's multiple comparisons test; *a* and *e* for $P < 0.05$; *b* and *f* for $P < 0.01$; *c* and *g* for $P < 0.001$; *d* and *h* for $P < 0.0001$.

Figure 1



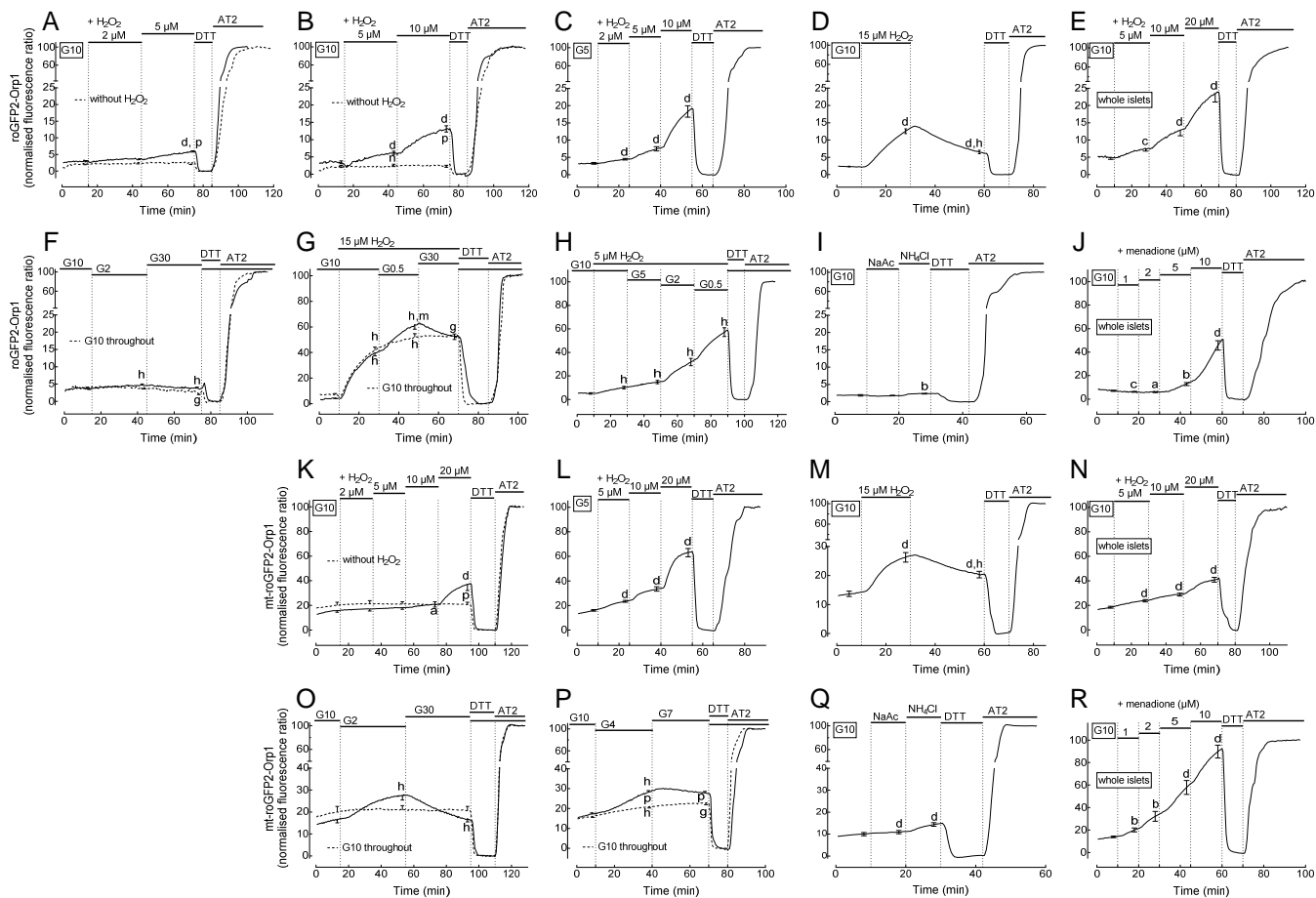


Figure 2

Figure 3

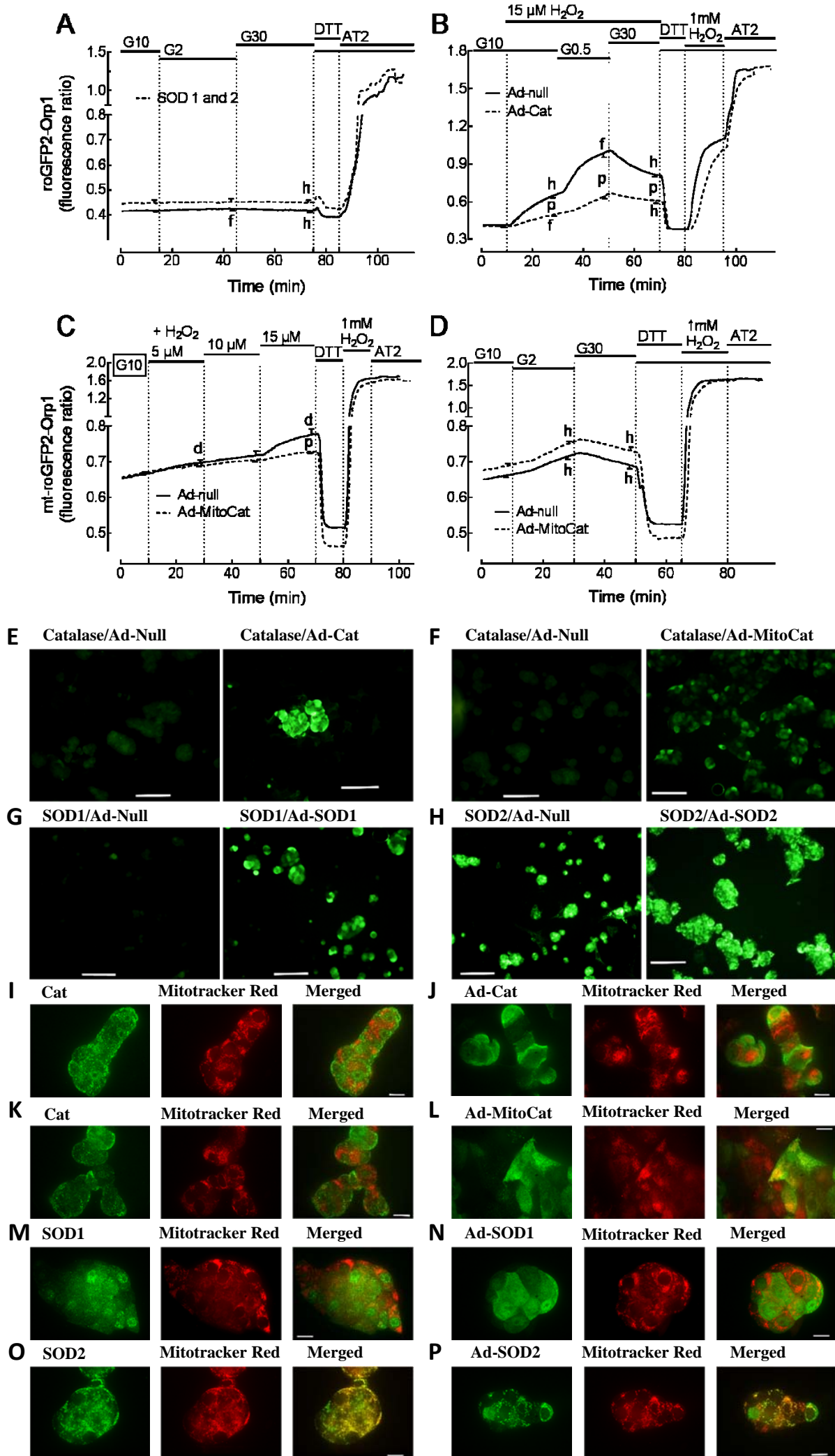


Figure 4

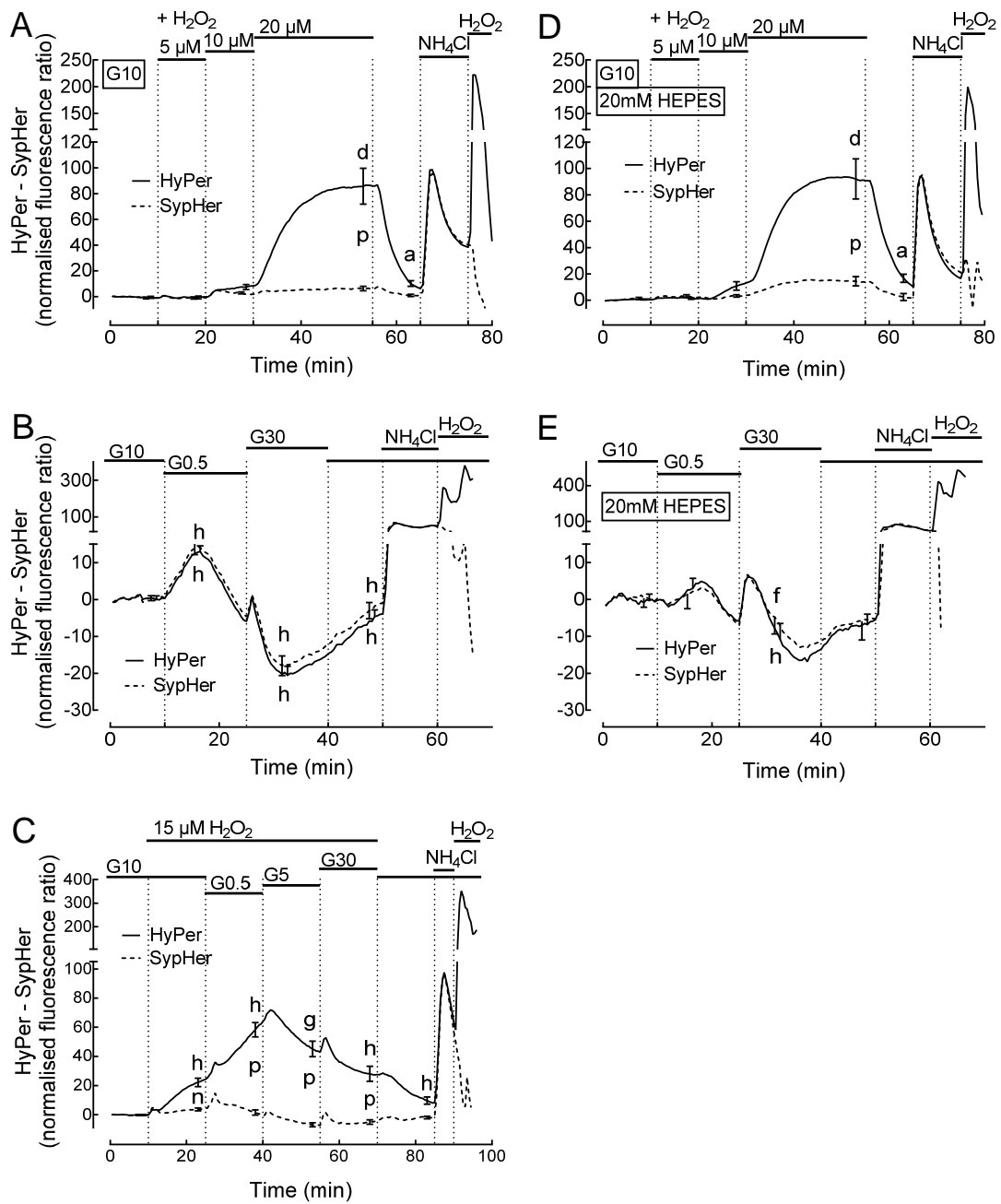
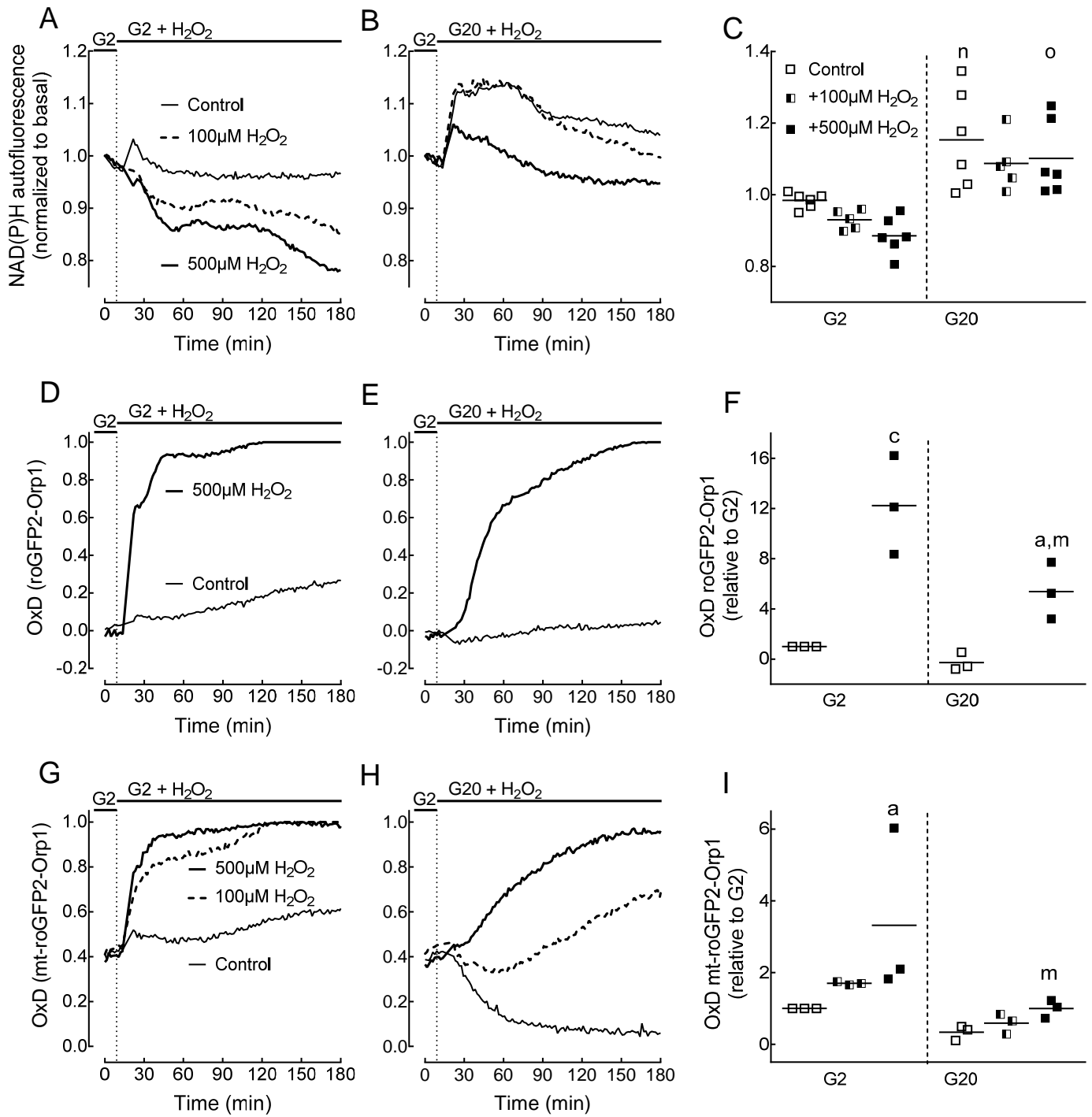


Figure 5



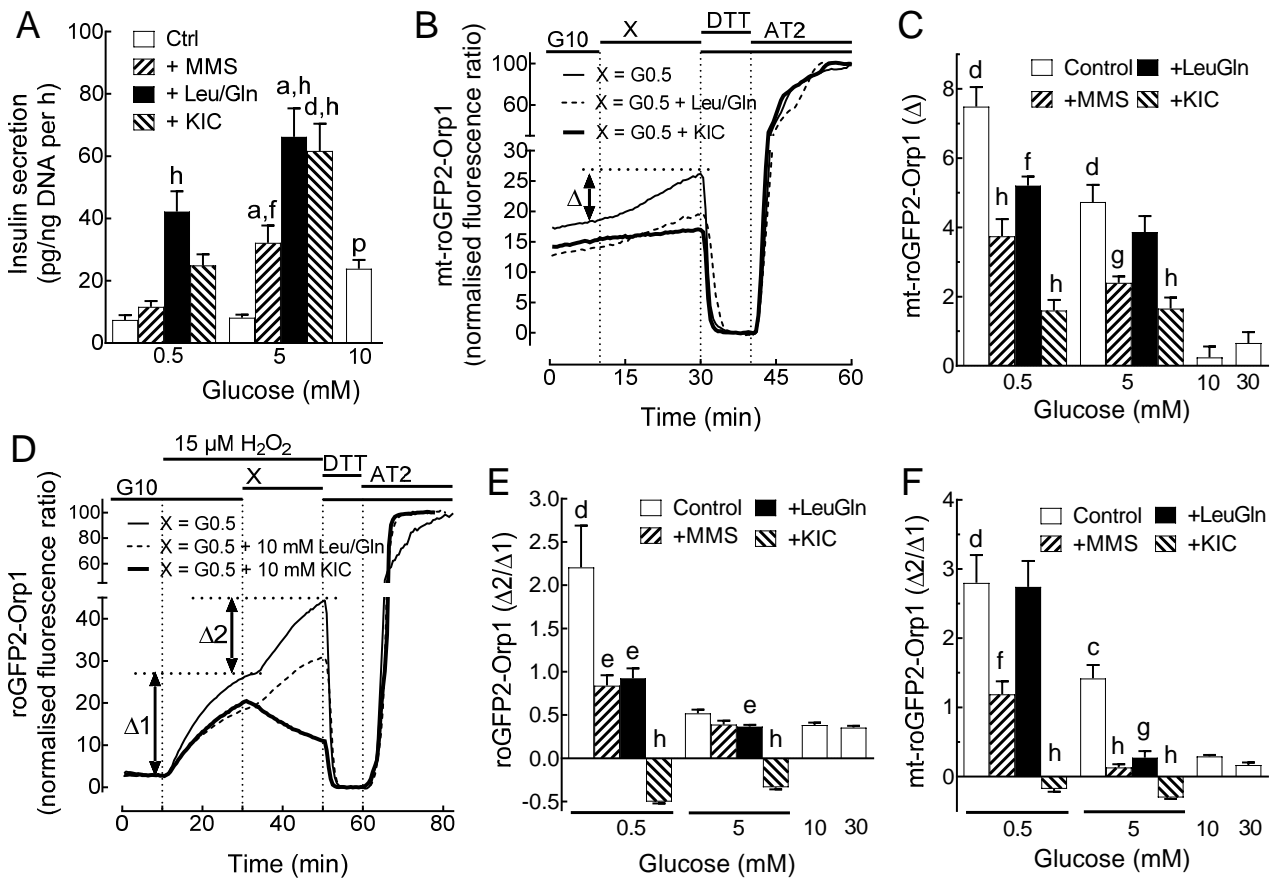


Figure 6

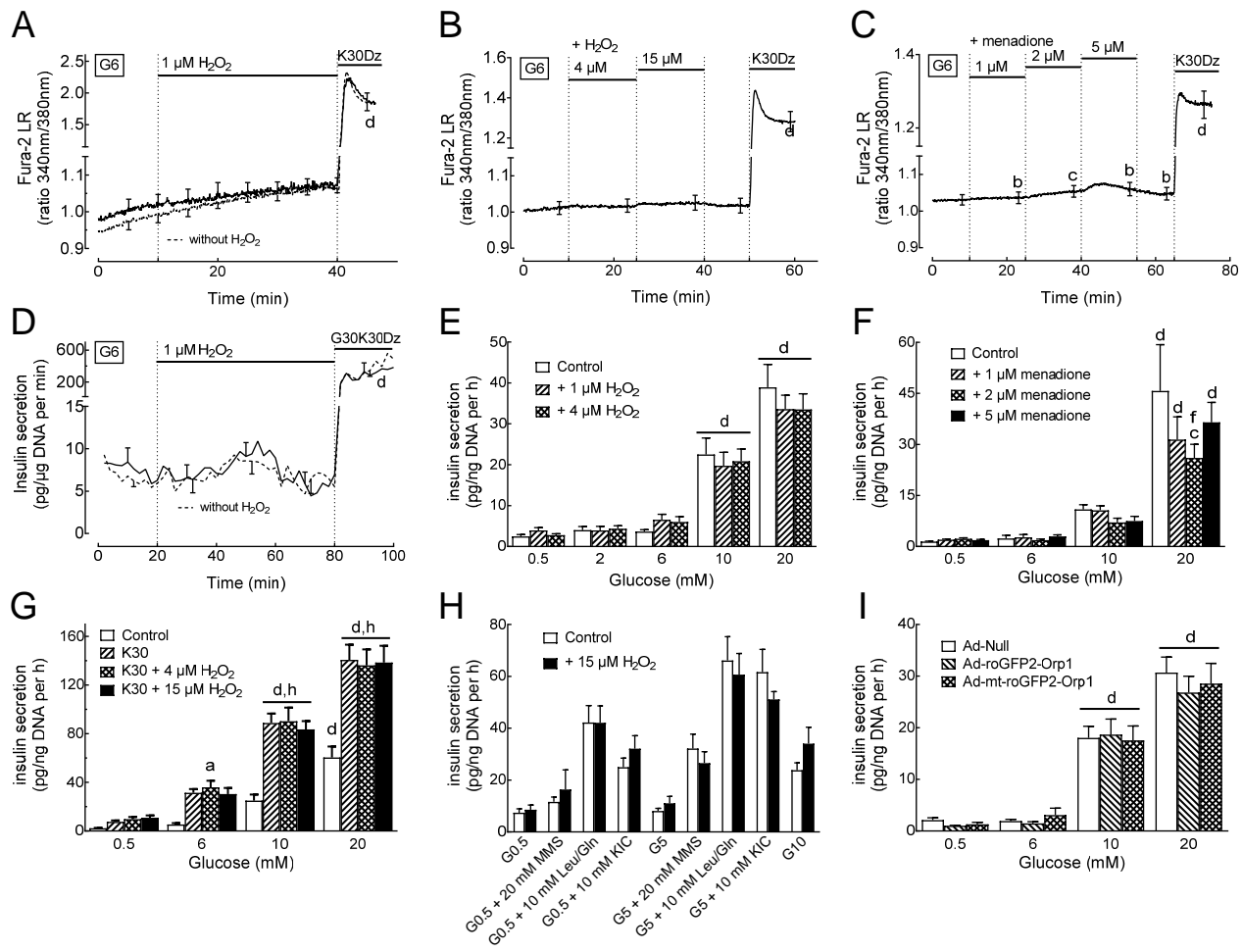


Figure 7